

PAPER • OPEN ACCESS

Long-term *in vitro* maintenance of plasma cells in a hydrogel-enclosed human bone marrow microphysiological 3D model system

To cite this article: Stefania Martini *et al* 2024 *Biofabrication* **16** 045005

View the [article online](#) for updates and enhancements.

You may also like

- [Multi-messenger Observations of a Binary Neutron Star Merger](#)
B. P. Abbott, R. Abbott, T. D. Abbott et al.
- [Relative biological effectiveness \(RBE\) and out-of-field cell survival responses to passive scattering and pencil beam scanning proton beam deliveries](#)
Karl T Butterworth, Conor K McGarry, Ben Clasie et al.
- [Cox Proportional Hazard Survival Analysis to Inpatient Breast Cancer Cases](#)
M. Nadjib Bustan, Arman, M.Kasim Aidid et al.

Biofabrication



PAPER

OPEN ACCESS

RECEIVED
16 October 2023

REVISED
22 April 2024

ACCEPTED FOR PUBLICATION
1 July 2024

PUBLISHED
12 July 2024

Original content from this work may be used under the terms of the [Creative Commons Attribution 4.0 licence](#).

Any further distribution of this work must maintain attribution to the author(s) and the title of the work, journal citation and DOI.



Long-term *in vitro* maintenance of plasma cells in a hydrogel-enclosed human bone marrow microphysiological 3D model system

Stefania Martini^{1,2,*} , Norman Michael Drzeniek^{1,2} , Regina Stark^{1,9}, Matthias Reiner Kollert^{1,3} , Weijie Du^{1,4,9}, Simon Reinke¹, Melanie Ort^{3,5}, Sebastian Hardt⁶, Iuliia Kotko², Jonas Kath^{1,4}, Stephan Schlickeiser^{1,7} , Sven Geißler^{1,3}, Dimitrios Laurin Wagner^{1,4,8} , Anna-Catharina Krebs^{1,2,4,10,*} and Hans-Dieter Volk^{1,2,4,10}

¹ BIH Center for Regenerative Therapies (BCRT), Berlin Institute of Health (BIH) at Charité—Universitätsmedizin Berlin, Berlin, Germany

² Institute of Medical Immunology, Campus Virchow-Klinikum, Charité—Universitätsmedizin Berlin, Corporate Member of Freie Universität Berlin, Humboldt-Universität zu Berlin, and Berlin Institute of Health (BIH), Berlin, Germany

³ Julius Wolff Institute, Campus Virchow-Klinikum, Charité—Universitätsmedizin Berlin, Corporate Member of Freie Universität Berlin, Humboldt-Universität zu Berlin, and Berlin Institute of Health (BIH), Berlin, Germany

⁴ Berlin Center for Advanced Therapies (BeCAT), Charité—Universitätsmedizin Berlin, Corporate Member of Freie Universität Berlin, Humboldt-Universität zu Berlin, and Berlin Institute of Health (BIH), Berlin, Germany

⁵ Department of Biology, Chemistry and Pharmacy, Institute of Chemistry and Biochemistry, Freie Universität Berlin, Berlin, Germany

⁶ Center for Musculoskeletal Surgery Charité—Universitätsmedizin Berlin, Berlin, Germany

⁷ CheckImmune GmbH, Berlin, Germany

⁸ Institute of Transfusion Medicine, Charité—Universitätsmedizin Berlin, Corporate Member of Freie Universität Berlin, Humboldt-Universität zu Berlin, and Berlin Institute of Health (BIH), Berlin, Germany

⁹ Current address: Bayer AG, Research & Development, Oncology Research, Berlin, Germany.

¹⁰ Shared senior co-authorship.

* Authors to whom any correspondence should be addressed.

E-mail: stefania.martini@charite.de and anna-catharina.krebs@bih-charite.de

Keywords: plasma cells, microphysiological systems, organ-on-a-chip, primary bone marrow, 3D culture, tissue engineering, regenerative medicine

Supplementary material for this article is available [online](#)

Abstract

Plasma cells (PCs) in bone marrow (BM) play an important role in both protective and pathogenic humoral immune responses, e.g. in various malignant and non-malignant diseases such as multiple myeloma, primary and secondary immunodeficiencies and autoimmune diseases. Dedicated microenvironmental niches in the BM provide PCs with biomechanical and soluble factors that support their long-term survival. There is a high need for appropriate and robust model systems to better understand PCs biology, to develop new therapeutic strategies for PCs-related diseases and perform targeted preclinical studies with high predictive value. Most preclinical data have been derived from *in vivo* studies in mice, as *in vitro* studies of human PCs are limited due to restricted survival and functionality in conventional 2D cultures that do not reflect the unique niche architecture of the BM. We have developed a microphysiological, dynamic 3D BM culture system (BM-MPS) based on human primary tissue (femoral biopsies), mechanically supported by a hydrogel scaffold casing. While a bioinert agarose casing did not support PCs survival, a photo-crosslinked collagen-hyaluronic acid (Col-HA) hydrogel preserved the native BM niche architecture and allowed PCs survival *in vitro* for up to 2 weeks. Further, the Col-HA hydrogel was permissive to lymphocyte migration into the microphysiological system's circulation. Long-term PCs survival was related to the stable presence in the culture of soluble factors, as APRIL, BAFF, and IL-6. Increasing immunoglobulins concentrations in the medium confirm their functionality over culture time. To the best of our knowledge, this study is the first report of

successful long-term maintenance of primary-derived non-malignant PCs *in vitro*. Our innovative model system is suitable for in-depth *in vitro* studies of human PCs regulation and exploration of targeted therapeutic approaches such as CAR-T cell therapy or biologics.

1. Introduction

Bone marrow (BM) is a semisolid tissue within the cancellous (trabecular) bone. It is a complex microenvironment, also called the BM niche(s), comprising different cell types (hematopoietic and non-hematopoietic), together with extracellular components as the extracellular matrix (ECM), and chemical and physical factors [1–3], traversed by a network of arterial and sinusoidal vessels [4–6].

The BM is the central organ for hematopoiesis and a safe harbour for mature long-lived immune cells, such as antibody producing plasma cells (PCs) [1, 2]. Primary producers of circulating antibodies of different immunoglobulins (Ig) classes, PCs are a central component of the body's protection against infection.

PCs arise from antigen-activated B cells, which differentiate into plasmablasts and mature into either short-lived or long-lived PCs, depending on their microenvironment [7]. Short-lived PCs are mainly formed in extrafollicular sites of secondary lymphoid organs and express first low-affinity IgM antibodies. Chronic/repetitive antigen exposition triggers germinal centre reaction that induces, with T cells help, an Ig class switch and affinity maturation of antibodies. Short-lived PCs leave the germinal centres and migrate to inflammatory sites and BM. Subsequently, after homing in specialized niches, they can differentiate into long-lived PCs. Short-lived PCs are responsible for the initial burst of antibody production during an acute immune response and rapidly die after its resolution, while long-lived PCs provide long-term immunity, e.g. against recurring infections [3, 7, 8]. Long-lived PCs continuously produce and secrete high-affinity antibodies into the bloodstream, conversely to memory B cells, which are quiescent and respond quickly to antigens upon recall [8].

Failure to induce sufficient antibodies after infection or vaccination is related to compromised immunity and morbidity. Further, after break of immune tolerance, miss-targeted self-reactive antibody secreting PCs contribute to chronic autoimmune diseases. Recently, it was demonstrated that patients with Common Variable Immunodeficiency, the most frequent primary immunodeficiency, characterized by insufficient antibody secretion, can be divided into subtypes. Although in some patients antibody synthesis could be recovered *in vitro* by adequate stimuli, in other patients, reconstitution was not successful due to failure of PCs

formation [9]. Lastly, PCs with genetic mutations are responsible for multiple myeloma (MM), the second highest incidence hematological malignancy, which remains incurable, despite increasing treatment options [10].

Consequently, PCs are of broad interest to various disciplines ranging from basic immunology to clinical immunopathology, from autoimmunity, over immunodeficiencies to oncology [11].

The mechanisms underlying the differentiation of short-lived PCs to long-lived PCs is poorly understood, albeit of utmost importance for the development of effective vaccines or other immunotherapies.

Major limitation in PCs investigation is due to PCs not being intrinsically long-lived and of difficult *in vitro* maintenance, as their survival relies on specific pro-survival stimuli provided by their natural niches in the BM or mucosal tissues, or at sites of inflammation [3, 7, 8]. PCs appear to reside *in vivo* in close contact within BM stromal cells, in particular reticular BM stromal cells, expressing VCAM-1 and CXCL12. These cellular stromal components are found in highly perfused zone surrounding sinusoidal and arterial network (perivascular niche), which provides a higher concentration of oxygen compared to other BM compartments [12]. Along with signals from cell–cell contacts, stromal cells, in concert with basophils, eosinophil and transient populations, are a necessary source of supporting cytokines. Among those molecular signals, production of IL-6 (cytokine associated with antibody titre maintenance due to its capacity to enhance PCs survival *in vitro*), B-cell activating factor (BAFF) and A proliferation-inducing ligand (APRIL) is crucial for the long-term survival of PCs [3, 8, 13]. Both APRIL and BAFF are ligands for BCMA on PCs, which signalling cascade enhances Mcl-1 anti-apoptotic expression, determining their long-lasting survival [3, 8, 14]. At the same time, BM's mechanical properties are characterized by an ample heterogeneity, as reflected by the lower stiffness near perivascular areas that contrasts to the higher stiffness in the endosteal space [15, 16]. The interaction between these niches is both dynamic and constant, enabling the physiological survival of each cell element.

The BM's microenvironment complexity exacerbates the limitations of conventional *in vitro* 2D culture for studying PCs, as it fails to mimic the essential signals from the surrounding cells and matrix properties that support cell survival and function [17]. Even MM cells are strictly dependent to their

microenvironment to survive. Primary derived MM cells in fact die in classic 2D monoculture in a short time (approximately 5 d) despite their malignant nature [18]. Consequently, most researchers resort to using immortalized cell lines, which have their own drawbacks such as altered expression of key PCs markers, signalling, and functionality [19]. 2D-cultures cannot reproduce BM's tissue structure and the intercellular interactions that are required for the maintenance of the primary cell phenotype *in vitro* [18, 19]. A possible solution is PCs encapsulation in 3D biomaterials to create a more representative microenvironment and tissue architecture *ex vivo*. Common 3D culture matrices include hydrogels, either as homogenous gels with cells resuspended in the matrix or as microporous scaffolds with cells seeded on top. These matrices can consist of bioinert polymers, such as polyethylene glycol, alginate, agarose, or aliphatic polyesters or intrinsically bioactive polymers such as collagen I, elastin, gelatin, or Matrigel® [20, 21].

Hydrogel 3D structures have been already used to test whether primary MM cells can be maintained *in vitro*. Proposed 3D microenvironments for MMs are commonly based on co-culture of malignant primary BM mononuclear cells, with or without supporting mesenchymal stromal cells (MSCs), in a range of diverse hydrogel compositions (e.g. collagen I, Matrigel®, fibronectin) [22]. Human immune system intricacy creates a considerable challenge to co-culture and integration in 3D models. In the BM, several immune cells subpopulations find themselves in different maturation phases, activation status and amount, based on physiological state of the examined subject. Standardized procedures for creating reliable platforms for MM are therefore still missing [22].

BM-on-a-Chip models, so far described in literature, are focused on achieving a BM-mimetic environment by assembling individual cellular components of the BM niche, such as MSCs and hematopoietic stem cells (HSCs) on artificial scaffolds to study survival, differentiation and proliferation of HSCs and their progenitors [4, 23, 24].

To the best of our knowledge, there exists no culture strategy—2D nor 3D—that allows long-term maintenance of primary, non-malignant human long-lived PCs *in vitro*.

In this study, we describe the development of a dynamic microphysiological BM platform (BM-MPS) that preserves the physiological survival niche of human PCs and enables *in vitro* long-term maintenance. We propose to employ a photocrosslinkable type 1 collagen HA hydrogel (Col-HA) [25] with tuneable mechanical stability to encapsulate primary human BM tissue. Additionally, we established first steps towards the transition from a static to a dynamic microphysiological system (MPS),

implementing a microfluidic organ-on-a-chip BM culture that includes constant fluid flow perfusion to resemble *in vivo* physiological conditions more closely. Thus, generating a 3D model that allows the long-term *in vitro* monitoring of non-malignant PCs phenotype and function. Our BM-MPS platform is not only a valuable tool for investigating the efficacy of new immune therapies, but also enables mechanistic studies of the recruitment and persistence of malignant cells or other BM-related pathologies in the human context.

2. Materials and methods

2.1. Human samples

Human BM samples (trabecular bone) were collected from 26 patients undergoing hip arthroplasty (supplementary figure S1, supplementary table T1).

2.2. Tissue sampling

All steps were performed in sterile conditions. The biological material received was assessed macroscopically to eliminate clearly necrotic, fatty, or clotted areas. Smaller pieces of BM were cut from the whole biological material and measured in terms of volume (length × width × depth) for later normalization for 100 cubic millimetres. These smaller samples were subsequently cultured or tested for *ex vivo* tissue characterization.

2.3. BM cell detachment

Ex vivo tissue (day 0) and cultured pieces (all timepoints considered in each condition) were treated to detach cells for flow cytometric analysis. Leftover material and BM pieces were twice resuspended in 20 ml and 5 ml respectively of detach buffer containing PBS (Gibco), 5 mM EDTA (VWR Life Science), 1% bovine serum albumin (Miltenyi). Gently inverted for approximately 20 times, the supernatant was collected through 100 μ m cell strainer. Collected cell suspensions underwent cold erylysis (Qiagen). Strained and resuspended in PBS containing 0.5% heat-inactivated FCS (Biochrom) detached cells were either seeded for human BM-stromal cells recovery or cells subset distribution assessment via flow cytometry on a Cytotflex LX device (Beckman Coulter).

2.4. Human BM stromal cells culture and conditioned media collection

Detached cells *ex vivo* not used for flow cytometry characterization were seeded in culture flasks (Corning Inc) with DMEM low-glucose basal medium (Sigma-Aldrich), enriched with 10% FCS, 1% penicillin/streptomycin (p/s, Gibco), and 2 mM L-alanyl-L-glutamine (Glutamax, Gibco). After 24 h

of incubation, flasks were washed with PBS to eliminate cells that grow in suspension and select the stromal compartment. Adherent cells were cultured until they reached 70%–80% confluency, washed with PBS and cultured with DMEM medium with reduced FCS (1%). After 24 h conditioned medium was collected and stored at -80°C for subsequent use in our optimized culture medium (OCM).

2.5. Agarose encasing

Sterile 4% low gelling temperature agarose (Sigma) in PBS (melting point $\leq 65^{\circ}\text{C}$; congealing temperature 26°C – 30°C) was melted at 80°C and lowered to 40°C before its use on the BM. 0.5–1 ml of melted gel was poured on each sampled BM fragment that needed inclusion and rested 5–10 minutes at 4°C to facilitate solidification of the construct.

2.6. Col-HA formulation and encasing

A previously described hydrogel consisting of type 1 collagen and hyaluronic acid (Col-HA) and suitable for 3D cell culture *in vitro* [25] was used to encapsulate the BM tissue. Briefly, telopeptide-intact methacrylated type 1 collagen (Advanced Biomatrix) reconstituted to 6 mg ml^{-1} and thiolated hyaluronic acid (HA, Advanced Biomatrix) reconstituted to 10 mg ml^{-1} in 0.1% Irgacure 2959 (Advanced Biomatrix) solution were mixed in a 2:1 volume ratio, then diluted in culture medium at a 1:1 volume ratio. The hydrogel was cast in 96-well membrane plate (Sigma-Aldrich) wells containing BM samples (static culture) or directly in the HUMIMIC Chip2 chambers (TissUse GmbH) (dynamic microphysiological culture, MPS) together with the tissue. Instantaneous photopolymerization was triggered by irradiating the gels with UV-A light (1.4 W cm^{-2}) for 3 s.

2.7. Gel characterization

Mechanical characterization for compressive modulus was performed using unconfined uniaxial compression testing (TestBench LM1 system, BOSE) with a compression rate of 0.016 mm s^{-1} until 15% strain, similar to the method previously described [26]. Compression testing data was analysed using a custom-made MATLAB (MathWorks) script to quantify elastic modulus (E) based on a 5% interval of strain that was located in the linear region of a measured stress-strain curve.

Rheological characterization was performed using a HR-20 rheometer (TA Instrument) in plate-plate configuration and TRIOS analysis software (TA Instruments) to quantify storage modulus (G'), and loss modulus (G'').

Compression testing and rheological measurements were performed at room temperature and after equilibration of hydrogel samples in PBS.

For scanning electron microscopy (SEM) of agarose and Col-HA structures, gel pellets of different concentrations of both gels were frozen at -80°C overnight after PBS equilibration, lyophilized, sputter coated with gold/palladium particles and imaged using a GeminiSEM 300 (Zeiss) at an accelerating voltage of 7.0 kV and a working distance of 7.0–7.9 mm [25]. Pore size diameter (long axis) of 10–20 pores for each acquired SEM image was measured with Fiji.

Proteolytic degradation of Col-HA hydrogels was determined in empty gels via incubation with a Collagenase P solution (Sigma Aldrich, *Clostridium histolyticum* 1.04 U ml^{-1} collagenase) at 37°C on a shaker plate. Progressive degradation was evaluated through weight measurements every hour, until total dissolution of the constructs in exam.

Swelling was defined as $\text{swelling rate (\%)} = ((M_1 - M_0)/M_0) * 100$ and quantified by measuring a hydrogel's mass using a calibrated balance (ABJ 220-4NM, Kern) directly after fabrication (M_0) and after incubation (M_1) for different periods of time (1, 6, 18, 24 h).

2.8. BM static culture

Native, agarose- or Col-HA-enclosed tissue pieces were cultured in 24-well tissue culture plates (Corning) for static evaluation of BM *in vitro* culture. Native and agarose conditions were cultured up to 7 d in RPMI (PAN Biotech) containing 10% heat-inactivated FCS (Biochrom), while Col-HA-encased pieces were cultured in RPMI (PAN Biotech) containing 10% heat-inactivated fetal calf serum (FCS, Biochrom) in 1:1 ratio with stromal cells conditioned medium previously described and enriched with recombinant human IL-6 (0.33 pg ml^{-1} , Biolegend), recombinant human APRIL (50 ng ml^{-1} , R&D System), sodium pyruvate ($50\text{ }\mu\text{l ml}^{-1}$, Gibco), 2-mercaptoethanol ($1\text{ }\mu\text{l ml}^{-1}$, Gibco), D-(+)-Glucose anhydrous ($4.4\text{ }\mu\text{g ml}^{-1}$, Sigma-Aldrich), 1% p/s (OCM) up to 14 d. Culture medium was half-exchanged on alternate days without disturbing the encased tissue. Collected culture supernatants were stored at -80°C for further investigations.

2.9. BM dynamic microphysiological culture (BM-MPS)

Col-HA-enclosed tissue pieces were cultured in HUMIMIC Chip2 dynamic MPS (TissUse GmbH) up to 14 d with OCM. Culture medium was half-exchanged on alternate days without disturbing the encased tissue. Collected culture supernatants were stored at -80°C for further investigations. $400\text{ }\mu\text{l}$ of dedicated medium was pumped through each circuit at 33 BPM, with 500 mbar of pressure and -500 mbar of vacuum.

2.10. Histological preprocessing, slides acquisition and analysis

Ex vivo (day 0) and cultured samples were fixed with 4% PFA (Sigma-Aldrich) overnight and demineralized with a solution of 20% EDTA (Sigma-Aldrich), to be subsequently processed and embedded in paraffin (Leica TP1020 Automatic Benchtop Tissue Processor). Hematoxylin (Sigma-Aldrich) and eosin (Sigma-Aldrich) stained slides (section thickness 4 nm) were scanned using the Nanozoomer SQ (Hamamatsu Photonics) 40x objective. To evaluate automatically and reproducibly the tissue slides, the open-source software QuPath [27] implemented with the MarrowQuant 2.0 script was used [28]. The algorithm provides the user the opportunity to quantify digitally five BM compartments (hematopoietic, adipocytic, interstitial-microvasculature areas, and bone).

2.11. Culture supernatant analysis

Culture supernatants were processed to establish soluble factors concentration and, Ig concentration and isotyping. Respectively, customized LEGENDplex™ Custom Human 6-plex panel (Biolegend) and pre-defined LEGENDplex™ HU Immunoglobulin Isotyping Panel (8-plex, Biolegend) were run following manufacturer's indication, data were collected on Cytoflex LX (Beckman Coulter). Concisely, LEGENDplex™ is a bead-based multiplex assay, with capture beads of different sizes and fluorescence, conjugated with analyte-of-choice specific antibodies. Following the principles of a sandwich immunoassay the beads are separated in sets based on their dimension and resolved by fluorescence intensities. Software for data analysis is provided by the company together with the kits.

2.12. Data analysis, statistics, and presentation

FlowJo Software (BD) was used to analyze flow cytometry data. QuPath's script MarrowQuant 2.0 was used to automatically quantify histology-stained tissue slides (code and tutorials available at <https://github.com/Naveiras-Lab/MarrowQuant2.0>) [28]. Compression testing data was analyzed using a custom-made MATLAB script. To measure SEM images pore sizes Fiji was employed. LEGENDplex™ Data Analysis Software Suite was used to analyze supernatant assays data. Graph creation and statistics were performed with Prism 10 (GraphPad). Assessment of statistical significance for normally distributed data values was performed with unpaired *t*-test with Welch's correction, repeated measurement one-way ANOVA with Geisser-Greenhouse correction, unpaired Brown-Forsythe and Welch ANOVA tests, and repeated measurements two-way ANOVA with Geisser-Greenhouse correction. Corresponding nonparametric tests were applied in case of non-normally distributed data with Mann-Whitney's test,

unpaired Kruskal–Wallis-Test, repeated measurements Friedman's test, and paired Wilcoxon test. Choice of statistic, post-hoc test and significant *P*-values are described under each graphic result representation. Images were created on BioRender.com and Affinity Designer.

3. Results

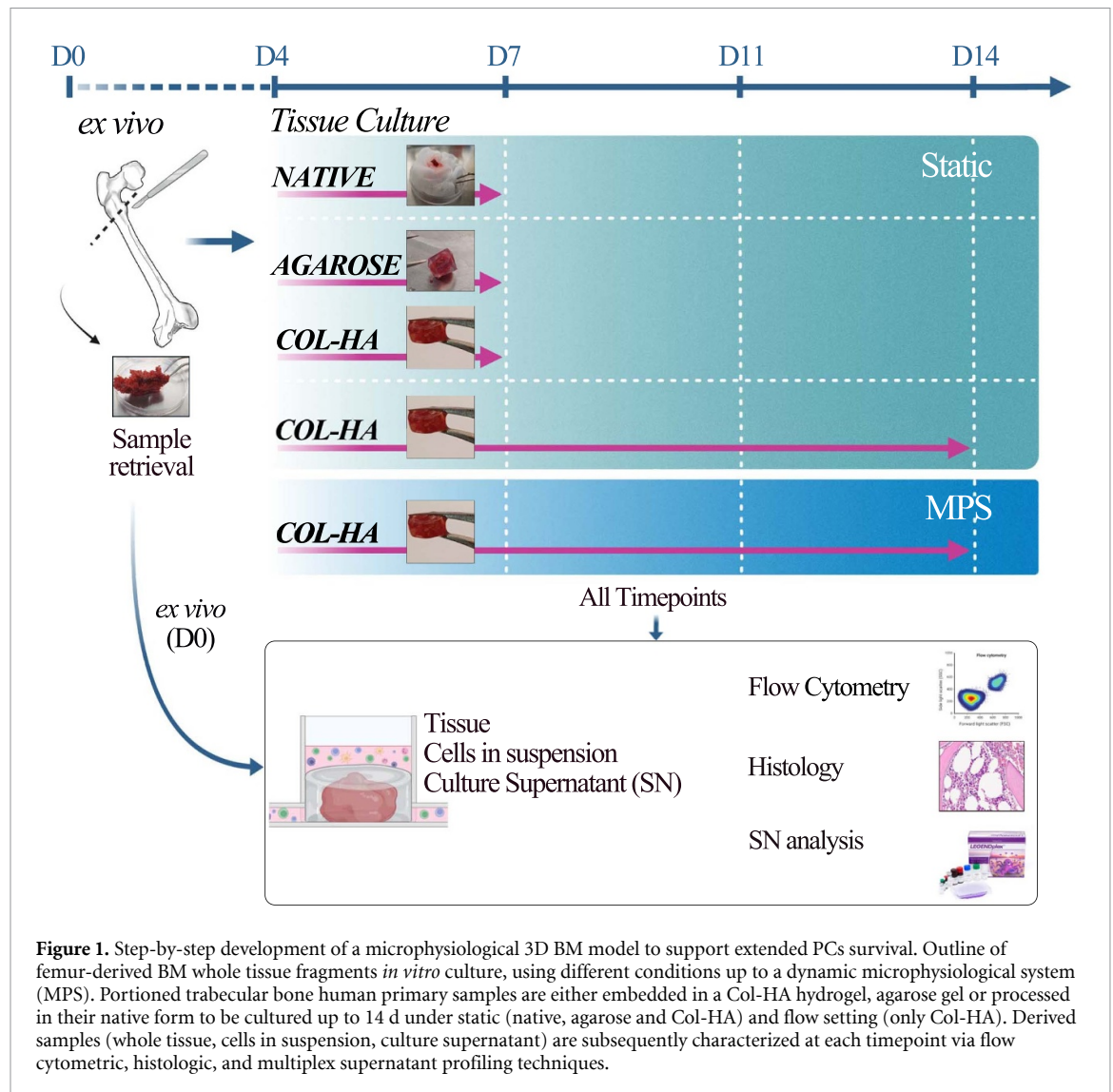
3.1. Development of a 3D human BM model on-a-Chip (BM-MPS)

Since the necessary cues that maintain PCs alive are not yet completely defined [7, 8], we chose to preserve the endogenous conformation of the *in vivo* BM. To this end, primary human femoral BM tissue was harvested from hip-replacement surgeries. To sustain long-term functional BM tissue *in vitro*, different setups were tested. Primary trabecular BM was cultured either in native form, embedded in low melting temperature agarose or enclosed in Col-HA hydrogel for mechanical support. The BM pieces were cultured under conventional stationary conditions (24-well tissue culture plate) or in the culture compartment of the HUMIMIC Chip2 (TissUse GmbH), providing a dynamic perfusion of the culture medium (figure 1). Preservation of the tissue integrity was tested by light microscopy. The maintenance of PCs in the cultured BM was analyzed at different timepoints (day 4, day 7, day 11, and day 14) by flow cytometry. In parallel, supernatant collection (SN) allowed us to further characterize the soluble portion of the *in vitro* culture micromilieu (Ig production—measured as a parameter for PCs functionality; as well as paracrine survival-inducing ligands) (figure 1).

Samples were obtained from a group of 26 donors, whose age varies between 51- and 85-years-old (mean age 68, balanced male/female sex distribution) (supplementary figure S1(a)). All donors underwent femur surgery due to coxarthrosis (homogenous distribution between left and right side) and presented a series of comorbidities not related to PCs impairment (supplementary figure S1(b)) (demographics detailed in supplementary table T1).

3.2. Characterization of *ex vivo* primary BM showed high donor variability

We used multi-colour flow cytometry to detect and quantify the immune cells subsets that populate the BM (figure 2(a)). Beside PCs (CD38+/CD138+/CD27+), we analyzed the samples for B cells (CD45+/CD19+) and T cells (CD45+/CD3+) (*ex vivo* and in culture), and for granulocytes (SSC/FSC) and HSCs (CD38-/CD3-/CD19-/CD34+) (only *ex vivo*) (supplementary figure S2 and supplementary table T2). All immune cell subsets were evaluated in their absolute numbers per 100 cubic millimetres (Abs/100 mm³) of each BM sample.



BM cellular density varied between donors up to 10-fold, ranging from $\sim 0.13 \times 10^6$ to $\sim 3.2 \times 10^6$ (figure 2(b)). We further observed strong donor-dependent differences in the composition of immune cell subsets. PCs were generally a rare subset, ranging from 0.08% to 1.41% of the analyzed cells (figure 2(c)). In general granulocytes represented the largest subset (47% mean, 10.45%–80.12% range) in most donors, followed by T cells (8.14% mean, 3%–21.85% range) and B cells (3.61% mean, 1.04%–15.34% range) (supplementary table T3).

3.3. Cultured tissue integrity can be achieved by BM encapsulation

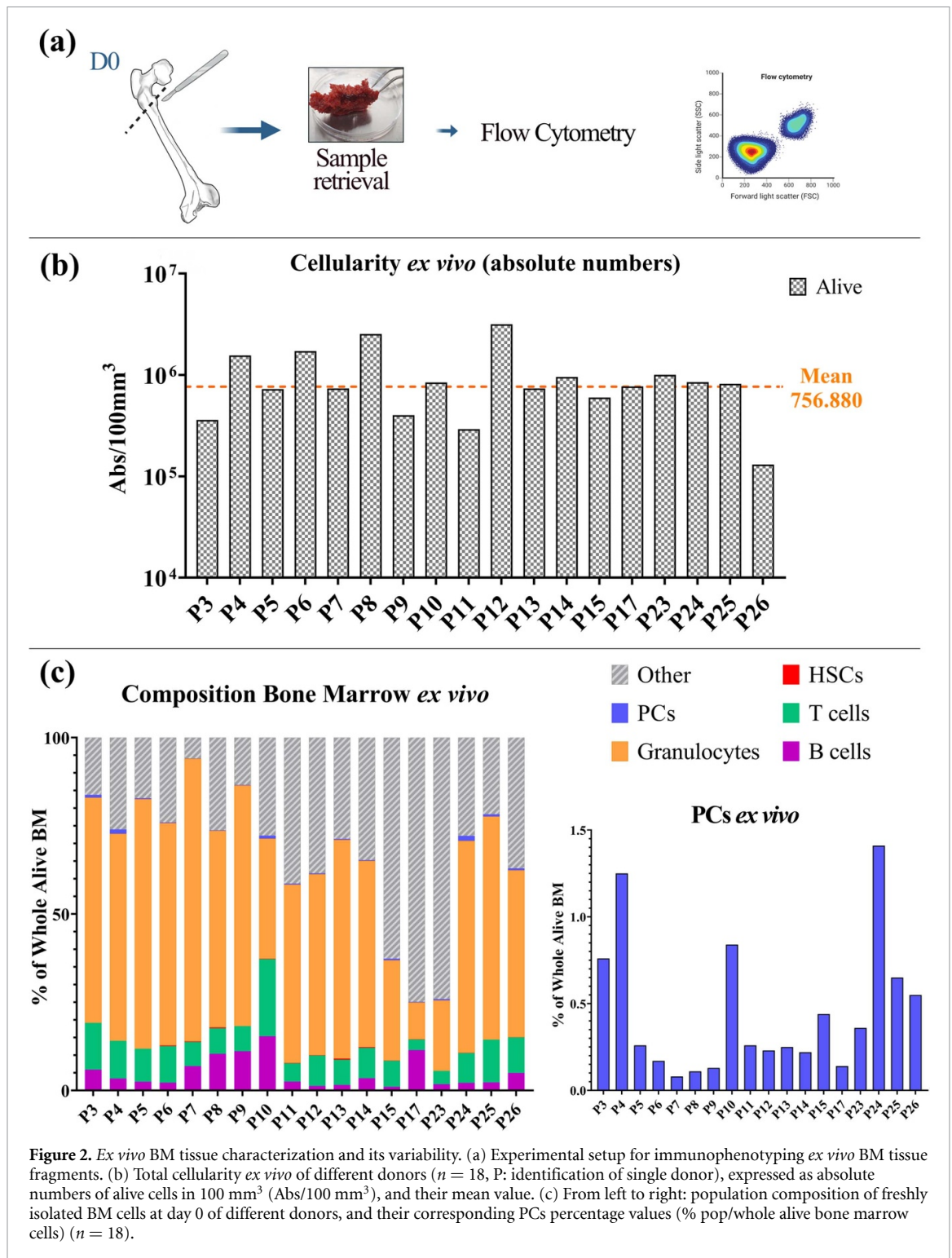
First, we analyzed the ability to retain tissue integrity in culture conditions by comparing BM in its native form to BM enclosed within a scaffold material. The testing was conducted in static culture wells filled with medium (24-well tissue culture plate).

Inspired by previous successful whole tissue cultures of different tissues [29, 30], and the documented

use of agarose gels in a range of different tissue engineering studies [31, 32], in an initial attempt to provide mechanical support, we embedded the whole tissue in a biologically inert low melting point 4% agarose gel. The experiment was performed in parallel to the static culture of the native tissue of the same donor (figure 3(a)).

Macro and microscopic observation of PFA-fixed scanned BM tissue H&E slides (*ex vivo*, day 7 native, day 7 agarose— $n = 3$ each condition), automatically analyzed via MarrowQuant 2.0 [28] (QuPath script) (figures 3(b)–(d)) (supplementary table T4), enabled us to follow the progressive deterioration of the native tissue when put in culture without an external support (figure 3(b)).

It was not possible to examine the BM composition of native tissue at day 7 due to the complete fragmentation of the remaining tissue. Conversely, 4% agarose encapsulation showed only slightly diminished hematopoietic fraction compared to the *ex vivo* fragment (figure 3(c)). Trabecular bone area appeared to be well preserved and not altered during



the culture process (figure 3(d)). Next, we tracked cellular relative survival rate of the PCs and the other immune subsets at day 4 and day 7 in tissue and supernatant compartment of both native and agarose tissue. Due to the variability of cell numbers within the BM as previously described, we observed the behaviour of PCs by normalizing the measured values towards day 0 *ex vivo* analysis (figure 3(e)). In both native and agarose-enclosed cultured samples, almost no PCs were alive after 7 d of culture. More

specifically, the mean normalized PCs survival rate after 1 week of culture was in native condition 0.81% (± 3.72 SD; 0.08%–9.2% range) and in agarose-enclosed condition 1.09% (± 1.37 SD; 0.09%–3.95% range). Analysis of tissue and medium supernatant samples of agarose-enclosed condition demonstrated heavily decreased survival of B cells and T cells within the first 4 d of culture; however, survival of the lymphocytes persisted at a low level between day 4 and day 7 (supplementary figure S3(a)). Notably, we found only

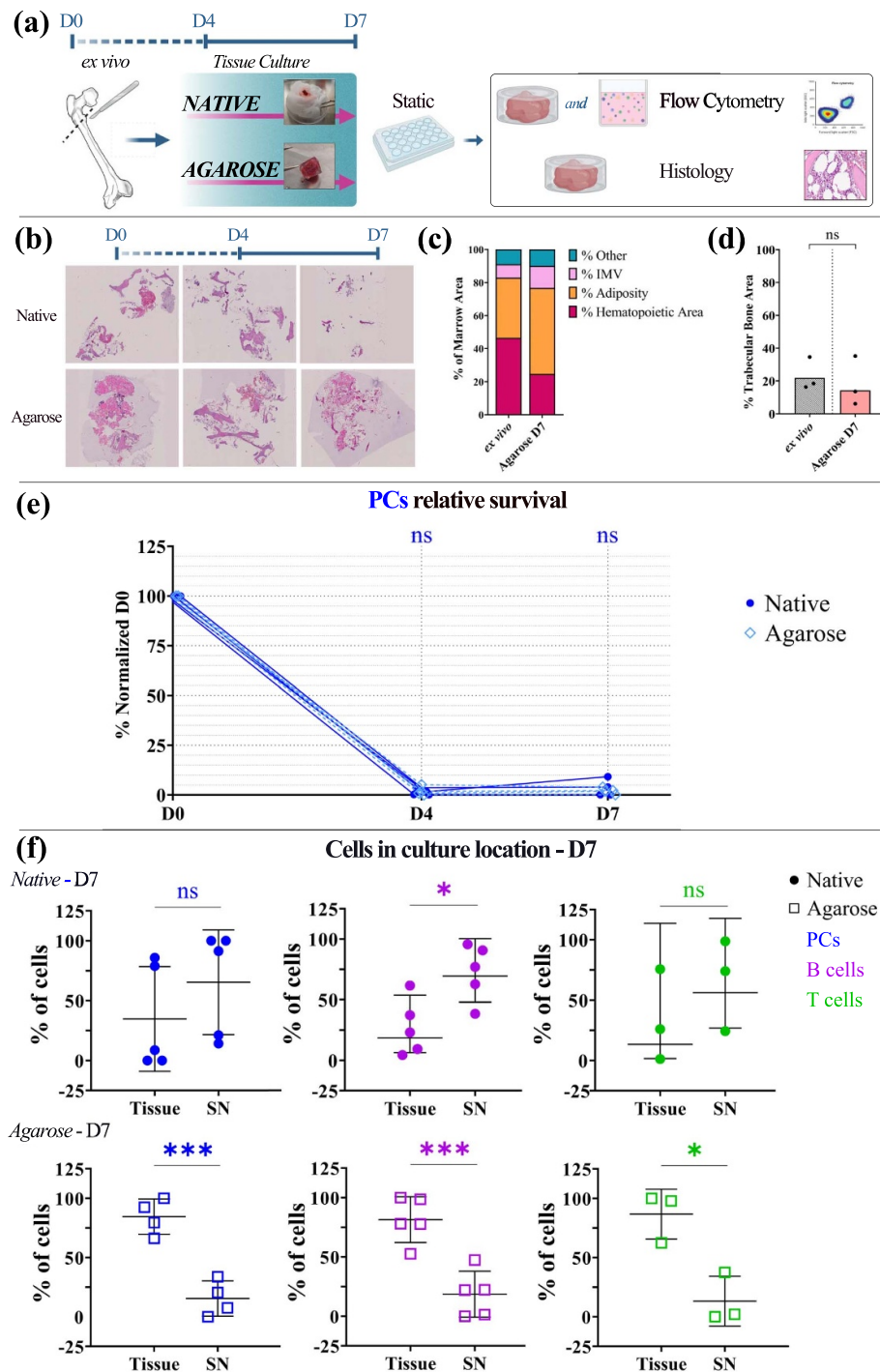


Figure 3. Native tissue and agarose embedding tissue culture evaluation under static condition. (a) Experimental setup for immunophenotyping of cultured BM tissue fragments (tissue and SN cells) and histology. (b) Pan cellular hematoxylin and eosin (H&E) stained scanned slides (magnification 40 \times) show progressive macroscopic deterioration of the tissue in culture without encasing (=native upper row), from left to right: *ex vivo*, day 4, day 7. Sharp contrast with agarose encased tissue (=gel lower row), from left to right: *ex vivo*, day 4, day 7. (c) Scanned H&E slides were automatically analyzed via MarrowQuant 2.0 (QuPath script). Summary of tissue composition in terms of hematopoietic area, adiposity, interstitial/microvasculature area ratio at different timepoints and conditions ($n = 3$). (d) More in detail data of trabecular bone area, compared to *ex vivo* ($n = 3$), on day 7 agarose embedded BM tissue ($n = 3$). Statistical analysis was performed by unpaired *t*-test with Welch's correction (ns: not significant), column height represents the mean value of each group. (e) Absolute numbers of alive PCs for 100 mm 3 of cultured BM (CD138+/CD38/CD27+) normalized to day 0. Survival trend up to 7 d ($n = 4$). Statistical analysis was performed by unpaired *t*-test with Welch's correction (ns: not significant). PCs non-normal distribution in agarose samples was statistically analyzed with nonparametric Mann-Whitney test (ns: not significant). (f) PCs, B cells and T cells distribution between in tissue residency versus supernatant circulation (% of mean values each culture condition), observed at day 7 (top row native, bottom row agarose-included) (day 7, % of mean values each culture condition). Statistical analysis was performed by unpaired *t*-test with Welch's correction (ns: not significant; ***: $p < 0.0002$; *: $p < 0.0332$). PCs non-normal distribution in native samples was statistically analyzed with nonparametric Mann-Whitney test (ns: not significant).

minimal counts of PCs, B or T cells in the supernatant of the agarose-encapsulated BM samples, indicating that BM cells were unable to freely exit the matrix (day 4 in figure 3(f); day in 7 supplementary figure S3(b)). Consequently, both these setups were abandoned.

3.4. Col-HA hydrogel as biologically relevant scaffold for BM culture

Embedding BM tissue allowed to preserve its morphological integrity (figure 3(b)).

The ECM of the physiological BM niche is composed of various type of collagens, HA, and proteoglycans such as fibronectin and laminin, in varying compositions between different BM compartments [19]. The bioactive environment within the BM niches provides cells with mechanical and biochemical cues that enable proliferation, differentiation, and survival [2, 4, 19].

Due to the poor survival of PCs in the 4% agarose gel (figure 3(e)), we hypothesized that a biologically relevant matrix, which more closely mimics characteristics of the *in-situ* microenvironment within the BM and mechanically supports the integrity of the native tissue, could improve PCs survival *ex vivo* (figure 4(a)). Further, we aimed to replace the temperature-dependent gelation of the agarose with light-triggered polymerisation to enable a more precise and robust encapsulation of the fragile BM tissue and therefore chose a UV-crosslinkable gel material. To better approximate the characteristics of the ECM composition in BM, the hydrogel mainly consisted of type 1 collagen and hyaluronic acid (Col-HA) [25]. Importantly, the Col-HA hydrogel was previously identified as favourable to maintain human BM stromal cells and promote their viability and function [25, 33]. The hydrogels are produced by a step-growth network of the methacrylated collagen (Col) and thiolated hyaluronic acid (HA) that forms through radical-mediated thiol-ene reaction and does not require any bioinert components for crosslinking. The resulting transparent hydrogel enclosed and maintained the integrity of the delicate BM tissue, allowing handling by forceps, despite being highly porous and permeable (figure 4(b)).

The mechanical properties vary greatly in the BM niche, ranging from the stiffer endosteal space to the softer BM [15]. For softer BM, different studies have previously reported an elastic modulus (E) of 0.25 kPa [15] and a storage modulus (G') of 220 Pa [16]. We aimed to use Col-HA gels with mechanical properties comparable to BM. Thus, we quantified elastic and rheological properties of different configuration of the Col-HA gels next. For 6, 2, and 0.5 mg ml⁻¹ configurations of Col-HA gels, E was measured at mean values of 4.3, 1.5 and 1.2 kPa, respectively (figure 4(c)), G' was measured at mean values of 547, 161 and 15 Pa, respectively (figure 4(d)), and G'' was measured at mean values of 14, 3 and 1 kPa (figure 4(d)). Consequently, we chose the Col-HA gels

in 2 mg ml⁻¹ configuration for further cell culture experiments as it showed E and G' comparable to values reported for BM in the literature. Notably, Col-HA 6 mg ml⁻¹, 0.5 mg ml⁻¹ presented here were deemed unfavourable for the cell culture setup (BM static and BM-MPS culture) due to their difficult handling in the production of enclosed BM samples, which lead to an increased variability in the culture settings. To provide a more complete characterization of the Col-HA material system, we next quantified porosity using SEM, degradation by enzymatic digestion, and swelling properties by mass change during incubation. SEM showed similar porosity for all three Col-HA configurations in the range of 60–131 μ m (figure 4(e)), which was in line with previously reported measurements [25]. Degradation measurements showed how Col-HA is subject by degradation when incubated with collagenase P. Higher concentration required longer incubation time, yielding to complete degradation after 12 h for 6 mg ml⁻¹ of collagen, 9 h for 2 mg ml⁻¹ and 6 h for the lowest collagen concentration of 0.5 mg ml⁻¹ (figure 4(f)). Swelling quantification showed that Col-HA gels in 6 and 2 mg ml⁻¹ configurations were stable and did not relevantly change in weight, contrasting the 0.5 mg ml⁻¹ configuration which showed substantial shrinking (figure 4(f)). The shrinking in the latter configuration likely was due to the lower concentration of collagen in the Col-HA mix, leading to incomplete crosslinking of the HA content, which may have result in de-swelling due to unlinked HA molecules diffusing out from the gel. For the 2 mg ml⁻¹ configuration, no macroscopic shrinkage was observed during 14 d of incubation, and no change in E was quantified between 1 and 14 d of incubation in PBS following hydrogel production (supplementary figure S4(f)), showing stable mechanical properties and no intrinsic degradability of the Col-HA gels.

3.5. BM-Col-HA platform supports the survival of PCs up to 14 d in culture

Col-HA hydrogel was already successfully tested for culture of human BM MSCs derived from the same category of samples used in the present study [25, 33]. We then tested whether this hydrogel would enable more physiological encapsulation of our trabecular BM, facilitating PCs survival and cell trafficking outside of the tissue (figure 5(a)). We achieved to encase the trabecular bone in Col-HA and proceeded to compare its integrity and relative cells survival rate after culture in both static and dynamic conditions (MPS: pump rate 33 BPM, imposed pressure 500 mbar). The Col-HA hydrogel maintained the BM fragments integer for up to 14 d, even when cultured under flow conditions (figure 5(b)).

The scanned BM tissue H&E slides (*ex vivo*, day 14 Col-HA static, day 14 Col-HA MPS— $n = 3$ each condition) were automatically analyzed as stated

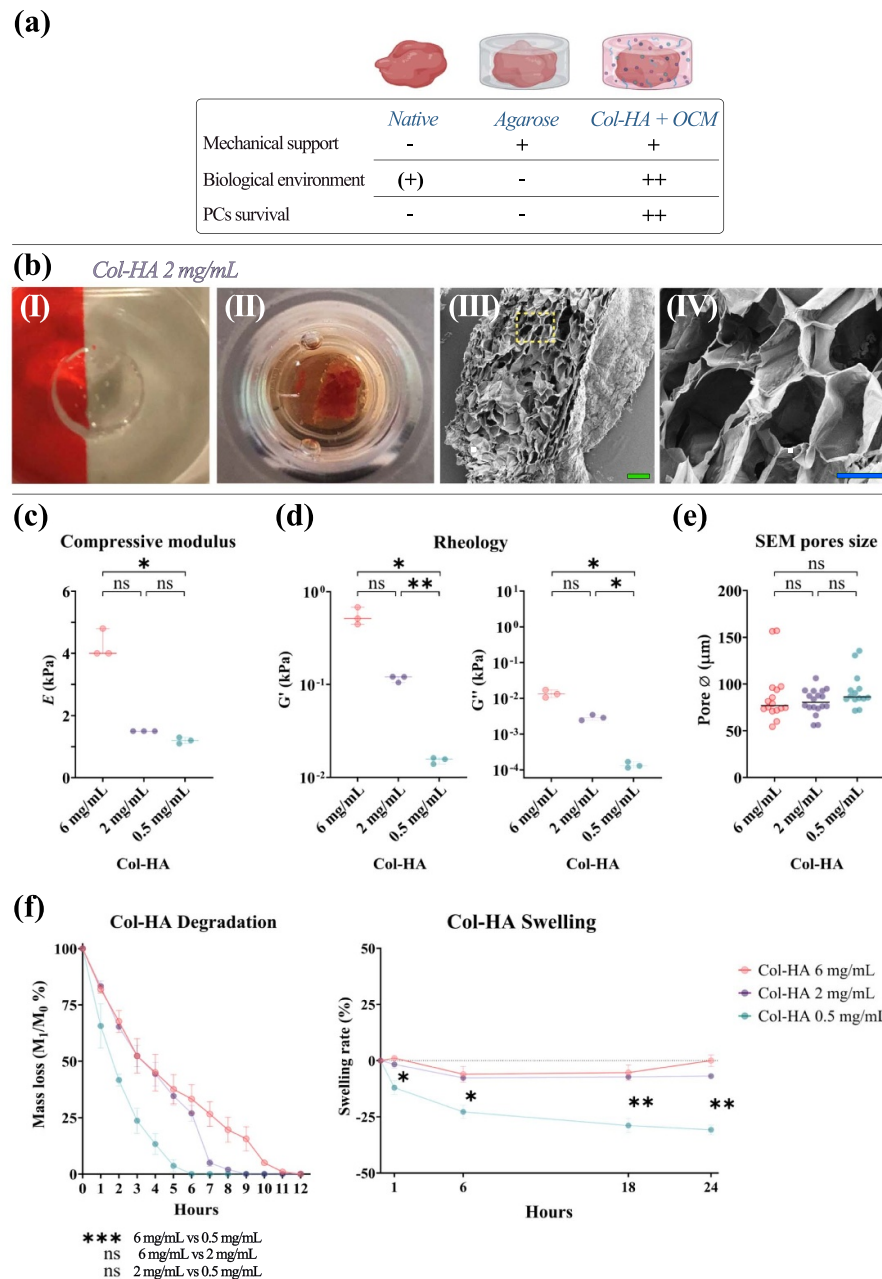
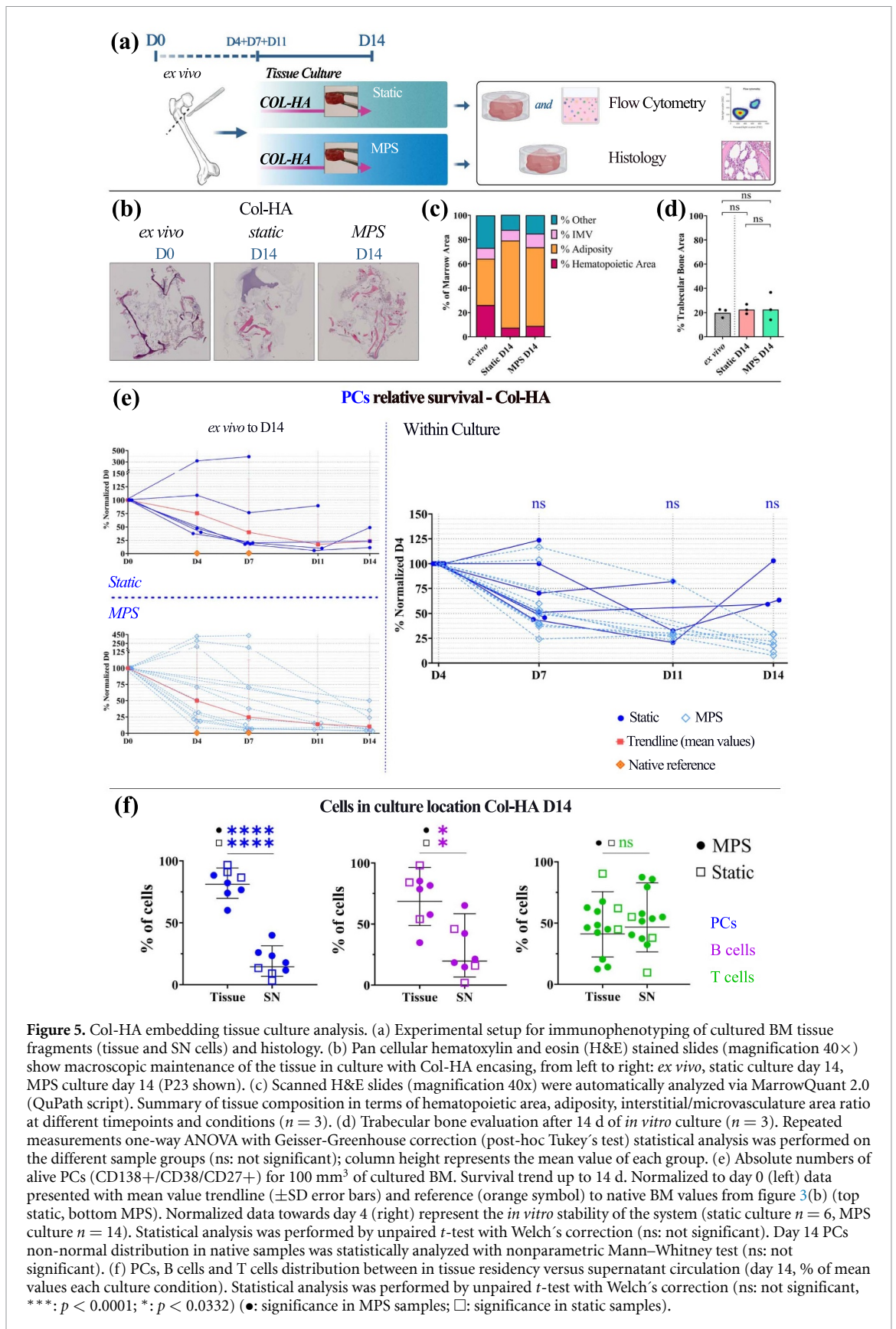


Figure 4. Col-HA hydrogel as biologically relevant casing for BM primary tissue. (a) Supporting qualities of agarose and Col-HA encasing solutions. (b) Col-HA is a self-supporting hydrogel (I) well suited to encapsulate the delicate BM (II). SEM of lyophilized Col-HA reveals a highly porous inner structure (III scale bar = 300 μm ; IV scale bar = 100 μm). (c) Compression testing was used to quantify E of Col-HA gels with different concentration ($n = 3$). (d) Rheometry was used to quantify G' and G'' for the Col-HA gel configurations ($n = 3$). (e) SEM pore measurement of fractured lyophilized gels (median pore size shown, $n = 2$). (f) Enzymatic degradability of Col-HA gel configurations tested by exposure to collagenase and quantified by mass loss percentage at different timepoints ($n = 3$). Statistical analysis of E and pore size were performed by unpaired Kruskal–Wallis–Test with Dunn’s post-hoc test. G' and G'' statistical analysis was performed by unpaired Brown–Forsythe and Welch ANOVA tests with Dunnett’s post-hoc test. Degradation test was analyzed with a repeated measurements Friedman test (Dunn’s post-hoc test). Swelling statistical analysis performed with repeated measurements ANOVA with Geisser–Greenhouse correction (Tukey’s post-hoc test). For all statistical analysis: ns: not significant; ***: $p < 0.0002$; **: $p < 0.0021$; *: $p < 0.0332$.

before (supplementary table T4). The hematopoietic fraction was slightly reduced compared to the *ex vivo* fragment, but without significant difference between static or dynamic culture conditions (figure 5(c)). Trabecular bone area was not altered in static and MPS culture compared to the *ex vivo* condition, corroborating the ability of the selected

encasing hydrogel to preserve general tissue architecture (figure 5(d)).

Next, we tracked cellular survival rate of PCs and other immune subsets at day 4, 7, 11 and 14 in both tissue and supernatant compartment of our Col-HA culture settings (figure 5(a)). Due to the variability of the PCs numbers in the starting material,



we normalized the PCs counts of different donors towards day 0 *ex vivo* absolute numbers (figure 5(e)). There was a significant decline of surviving cells in the passage from the *ex vivo* tissue excision to

the *in vitro* culture for all samples in the first days of culture (figure 5(e), left graphs—normalized to day 0). Once in culture, the PCs survival decreased at a slower rate, therefore we additionally normalized

the data towards day 4 to better evaluate the stability of the culture (figure 5(e), within culture observation—normalized to day 4). However, we could observe PCs maintenance up to 14 d after isolation. Over the two weeks, PCs frequency in the tissue continuously declined, with a mean of 32% (± 8.9 SD; 22%–44% range) of PCs remaining under static conditions and a mean of 10% PCs (± 17 SD; 4%–50% range) remaining in the MPS at day 14 (normalized to day 0). Regarding in culture maintenance (normalized to day 4), detected PCs survival appear more stable, with a mean of 73% under static conditions (± 20 SD; 59%–103% range) and of 17.5% in MPS (± 7.5 SD; 8%–29% range). Similar decline in alive cell numbers was observed for B cells and T cells extracted from the tissue sample of the Col-HA (supplementary figure S5(a)). In addition to the tissue analysis, we evaluated how many cells could be detected in the supernatants of the Col-HA enclosed BM and compared it to the numbers found in the tissue. We observed a preferential PCs survival in the tissue regardless of static/dynamic culture and only a minimal number of alive PCs in the supernatants at both early (day 4) and late (day 14) timepoints (figure 5(f), supplementary figure S5(b)). In contrast to PCs, B cells and T cells could be detected at comparable numbers in the tissue and the supernatant (figure 5(f), supplementary figure S5(b)).

3.6. PCs survival correlates to accumulation of immunoglobulin in supernatant of cultured 3D tissues

PCs secrete about 10^3 antibodies per second ($=2$ ng/day) [7]. Therefore, we evaluated ongoing production of antibodies in our 3D BM model through a dedicated multiplex human Ig isotyping panel from day 4 to day 14 ($n = 4$). We detected a mean increase of total immunoglobulin (TIg) in both static (2-fold) and in the MPS (1.4-fold) (figure 6(b)). Given TIg long half-life (ca. 3 weeks) [34] and the decrease of total PCs counts (figure 5(e)), the concentration increase indicated active production of TIg in our culture system, thereby validating PCs maintenance from a functional perspective across all different Ig isotypes (figure 6(c)). No significant differences were observed between static and MPS culture conditions for the different Ig subclasses.

3.7. OCM conditioned medium impact on survival factor expression

To support and potentially enhance PCs survival in our model, we have developed an optimized culture medium. Beside the use of human BM stromal cell conditioned medium (hBM-stromal CM) produced in batch from our same BM donors, factors as APRIL, IL-6 and glucose are added to enrich basal RPMI medium (see Materials and Methods). We investigated collected culture supernatants (SNs) of Col-HA-encapsulated BM samples from static and MPS OCM

cultures (day 4 to day 14), with a customized multiplex growth factor and cytokine panel. Given their importance for PCs survival we decided to focus our analysis on testing APRIL, BAFF, CXCL12, VCAM-1, VEGF, and IL-6 (figure 6(d)). We saw a general stability of the concentration of all the molecules, beside VEGF, up to day 11, regardless of static or MPS culture condition. APRIL and BAFF both promote proliferation and survival of PCs through the upregulated receptor BCMA [7, 8]. The enrichment of our OCM with APRIL seem to maintain stable levels throughout the BM *in vitro* culture, while BAFF, even if not added, is still present and apparently produced by the cells in the model with a higher concentration in the flow-stimulated construct. A key factor for PCs homing and maintenance in the niche, CXCL12, is expressed by a rare population of CXCL12-abundant reticular cells at constant low levels (~ 10 pg ml⁻¹). VCAM-1 is constitutionally expressed in perivascular stromal cells which are found in close proximity to BM vessels and, an important regulator of cell homing. In our system we saw a steady decrease of VCAM-1 which may or may not be related to loss of endothelial cells, stromal cells or both compartments. VEGF, well-known proangiogenic factor, shows an inverse trend in relation to VCAM-1. IL-6 was added at low concentrations (0.33 pg ml⁻¹) to stimulate PCs Ig production and remains present at an average concentration range of 10–20 ng ml⁻¹, which was observed in a previous study to increase the *in vitro* survival of PCs, in combination with BAFF and APRIL [23].

4. Discussion

In this paper, we introduce a novel approach to facilitate PCs survival *ex vivo* by enclosing primary trabecular human BM in a hydrogel. The selected pore sizes, stiffness, remodelling capabilities of the designed hydrogel allowed PC-supporting medium supplements to diffuse and leukocytes to migrate outside the BM tissue samples. Alive PCs and immunoglobulin production was detected at least up to 14 d in both static and MPS cultures, which exceeds previously published lengths by 4–7 times [7, 8, 35–37]. We then could establish an *in vitro/ex vivo* model for (patho)physiological studies and testing of novel therapeutics targeting PCs.

The extended survival of some functional, Ig-producing PCs and the maintenance of PC-supporting factors, such as APRIL, BAFF, and IL6, found in the BM tissue supernatants suggest that our approach retained certain necessary physiological cues of the BM. The downward trend observable at day 14 might indicate suffering of the whole model with consequent decline of total cell numbers.

It would be of importance to have standardized, reliable PCs and MM models that can mimic the *in vivo* microenvironment [22]. More in general,

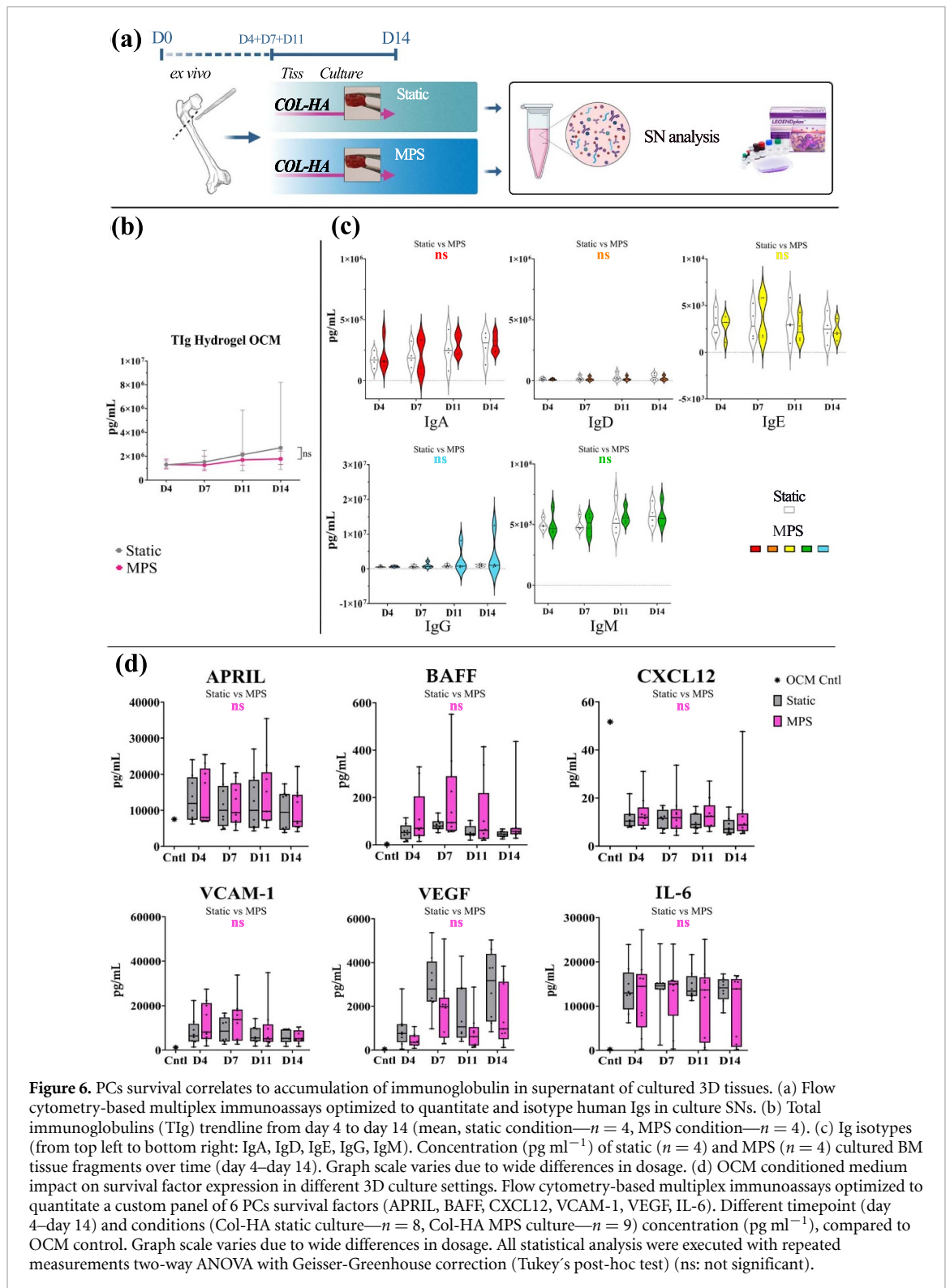


Figure 6. PCs survival correlates to accumulation of immunoglobulin in supernatant of cultured 3D tissues. (a) Flow cytometry-based multiplex immunoassays optimized to quantitate and isotype human Igs in culture SNs. (b) Total immunoglobulins (Tlg) trendline from day 4 to day 14 (mean, static condition— $n = 4$, MPS condition— $n = 4$). (c) Ig isotypes (from top left to bottom right: IgA, IgD, IgE, IgG, IgM). Concentration (pg ml^{-1}) of static ($n = 4$) and MPS ($n = 4$) cultured BM tissue fragments over time (day 4–day 14). Graph scale varies due to wide differences in dosage. (d) OCM conditioned medium impact on survival factor expression in different 3D culture settings. Flow cytometry-based multiplex immunoassays optimized to quantitate a custom panel of 6 PCs survival factors (APRIL, BAFF, CXCL12, VCAM-1, VEGF, IL-6). Different timepoint (day 4–day 14) and conditions (Col-HA static culture— $n = 8$, Col-HA MPS culture— $n = 9$) concentration (pg ml^{-1}), compared to OCM control. Graph scale varies due to wide differences in dosage. All statistical analysis were executed with repeated measurements two-way ANOVA with Geisser-Greenhouse correction (Tukey's post-hoc test) (ns: not significant).

the capacity to approximate the physiology of a tissue microsystem, will determine the correct establishment of the 3D culture as well as the ability of the system to respond correctly to *in vitro* imposed stimuli. In contrast to previous endeavours which deconstructed the BM tissue and selected specific cell subpopulations to coculture with PCs in conventional 2D-systems [8, 35, 37], our approach exploits

the complete 3D-architecture including all its cellular and extracellular components. The ideal model should provide the ability to identify key factors regulating PCs survival, such as cell–cell interactions, cell–matrix interactions and cell receptors. To reach this last mentioned aspect, a 3D model should consider and comprise many aspects, like proper nutrient and molecular diffusion, oxygen gradients, cell

adhesion points, mechanical properties, vascularization. All this while allowing cells to normally behave in terms of proliferation, differentiation, and trafficking. At the present time, such complex endeavour still needs to find resolution in the BM 3D tissue field.

The advantage we can propose with our model choice relies in trying to preserve all the cues already present *in vivo*, and all the necessary cells in culture (physiologically represented in terms of different subset and numbers), giving us a higher chance of getting closer to an *in vivo*-like situation.

The first necessary element to achieve BM tissue *in vitro* maintenance is the use of a biorelevant encasing solution. When considering agarose gels for our initial efforts we knew about their widespread use in research as well as medical science [31, 32]. As bioinert, low cost, stiff material it has also been used in other 3D tissue engineering applications [31, 32], but the characteristic that most have been exploited are the lack of attachment sites for cells. This aspect, together with high stiffness is known to serve as impediment to cell migration [38], incapability of swelling, and non-degradability by human enzymes (lack of by cells in culture) separates broadly the agarose gels from Col-HA ones. To confirm our choice of Col-HA over agarose, we also included in our investigation different compositions of agarose gels (4%, 1%, 0.25%) (supplementary figure S4). For agarose 4%, we quantified E at 156 kPa and G' at 39 kPa (mean values, supplementary figures S4(c) and (d)), which are substantially different from previously reported mechanical properties of the physiological BM niche ($E = 0.25$ kPa, $G' = 220$ Pa) [15, 16]. A lower concentration of agarose (0.25%) showed mechanical properties E and G' similar to Col-HA 2 mg ml⁻¹ ($E = 1.4$ kPa, $G' = 718$ Pa; mean values, supplementary figures S4(c) and (d)). However, agarose 0.25% is difficult to manage as encasing solution as it easily gets disrupted during handling and is difficult to use in long-term cultures. Another disadvantage of the agarose gels used in this study was their lack of cell adhesion motifs and interaction anchoring points, which likely prevented to present a relevant physiological environment to the encapsulated tissue with cells [31, 38]. Together, these observations help explain the inadequacy of the used agarose gels for the described culture system and corroborate the need to use biorelevant hydrogels like Col-HA for high-complexity 3D culture systems. Col-HA gels with components and mechanical properties resembling characteristics of physiological BM tissue, but not agarose gels, enabled PCs survival and trafficking of immune cells (figure 5 and supplementary figure S5).

Despite our best effort to retain the tissue in its *ex vivo* form, we observed a drop in PCs survival in the first 4 d, with the residual PCs decreasing at a lower rate between day 4 and day 14 in most donors (figure 5(e)). Similar declines in cell survival were

also observed for most other cell types monitored, including B and T cells (supplementary figure S5(a)). The strong initial decline in PCs survival may be related with the traumatic manipulation to create BM samples for subsequent enclosure and sub-culture, which may lead to sheer stress and the secretion of pro-apoptotic signals [39, 40]. However, consecutive PCs decline observed in our system may be related to other differences to the BM *in vivo*, that can directly or indirectly hamper PCs survival, such as the failure to maintain cell types necessary to support PCs.

The vasculature supports BM organization *in situ* by creating niches with gradients of oxygen and nutrients around the capillaries [6], but it also promotes in-/efflux of immune cells, cytokines, and antibodies. In contrast, nutrient supply and gas exchange in our system is primarily regulated by the culture-medium and diffusion from the surface of the culture chamber. While providing a platform in which immune cells can circulate freely following the emulated pulsating flow, use of microfluidic device HUMIMIC Chip led to lower PCs absolute survival and, while maintain functionality, minor Ig production when compared to its static counterpart. However, we recognized an improvement in PCs' survival also in the BM-MPS, when compared to classical culture (native condition) (figures 3(e) and 5(e)).

In both native and agarose cultured samples almost no PCs were alive after 7 d of culture; therefore, both these setups were subsequently abandoned and, more specifically, after 1 week of culture, the mean of PCs survival rate for normalized to day 0 native sample was of 0.81% (0.08%–9.2% range). Agarose cultured samples PCs were detected as 1.09% (mean value, day 0 normalization, range 0.09%–3.95%). If we confront these values with the ones regarding MPS, we could notice that on day 7 PCs alive in MPS amounted to 30-fold times more than native (day 7 MPS, mean: 75%). If we want to compare the lowest timepoint of PCs survival in the MPS we would see almost 13-fold increase compared to classical survival of non-malignant PCs *in vitro* (day 14 MPS, mean 10%). These results show a defined improvement and a potential first step towards implementing a fully functioning MPS BM system. Future studies may alternatively explore vascularization induction in our model, which may supplement the hydrogel's capacity for cellular migration with the ability to modulate oxygen levels and nutrients through the intricate *in vivo* vasculature of the BM.

Many different cell types have been associated with long-term PCs survival, such as BM stromal cells, including osteoclasts [7, 8, 41], but also activated immune cells, including short-lived granulocytes [8, 42, 43]. In this study, while systematically include *ex vivo* all these different cell subsets in culture, we used specific multi-color flow cytometry panel to focus on elucidation of the relative survival of PCs,

B and T cells at different timepoints. Future studies may be supplemented by more in-depth analysis of the cellular composition of our BM model with advanced single cell analysis technologies, such as CITE-seq/scRNA-seq [44, 45] which may provide insights into whether the loss of specific (rarer) cell subsets precede PCs decay in our system. Such results would be instrumental to propose hypothesis-driven changes to optimize medium compositions to extend PCs survival or change the composition of the hydrogel, to modulate stiffness and pore sizes. Additionally, such specific analysis would provide us with an overview on which phenotypes of PCs, out of their heterogeneous pool, thrive in our MPS and if their expression profile is modified in any way when observed against their *ex vivo* counterpart.

The 3D BM construct will serve as non-malignant tissue control, tissue destination of tumour metastasis as well as location of primary tumours such MM. The present model could be already used to investigate cell-based immunotherapies against PCs, such as CAR-T cells, or bispecific CD3-engaging antibodies [46, 47].

5. Conclusions

In summary, our study results show the positive influence of primary whole BM niche maintenance *in vitro* on PCs survival. Architecture and function of BM was preserved by encasing primary human tissue harvested during femur surgery in a biologically relevant biopolymer matrix. As the necessary cues for maintenance of PCs survival are not yet completely defined, an advantage of our chosen approach lies in the preservation of the integrity of the *in vivo* BM microanatomy and niche composition. Despite the high variability in donor immune cell composition in the biopsies, the combination of Col-HA encapsulation and BM-supporting culture medium allowed to maintain the complex organization of the native BM niche and led to prolonged PCs maintenance *in vitro*. In contrast, survival was not achieved in a bioinert agarose gel. This study thus exemplifies how biomaterials can play a role in preserving functional tissue *ex vivo* beyond simple mechanical support.

On one hand, this *in vitro* BM model could be used to study the biology of non-malignant, human PCs and the necessary cellular components, soluble factors or physical cues necessary to support their long-term function and survival. On the other hand, this work represents a new tool for translational work on PCs-targeted therapies. The implementation of adaptive immunity with homing/migration and effector function of T and B cells in dynamic 3D organ systems would be of great scientific value, as it would raise exploratory preclinical studies on the pathogenesis of immune diseases as well as on mechanisms of action of new innovative therapeutic approaches to a

new level—saving animal experiments and simultaneously improving informative value.

Data availability statement

Data is contained within the article or supplementary material. Further data is available on request.

All data that support the findings of this study are included within the article (and any supplementary files).

Acknowledgments

The authors would like to express their gratitude to the bone marrow donors and to Antje Blankenstein, Johanna Penzlin, Kerstin Mika and Dag Wulsten (Charité Universitätsmedizin Berlin) for their technical assistance.

Conflict of interest

The authors declare no conflict of interest related to this specific work. It should be noted that the authors used commercially available chips from TissUse GmbH, a SME that is a partner of the two EU consortia ReSHAPE and geneTIGA.

Author contributions

S M designed this study, planned, and performed experiments, analyzed results, interpreted the data, and wrote the manuscript. N M D contributed biomaterials methodology, helped in study design, interpreted the data, and edited the manuscript. R S designed this study, planned, and performed experiments, analyzed results, interpreted the data, and edited the manuscript. M R K performed experiments, analyzed results, interpreted the data, and edited the manuscript. W D analyzed results, interpreted the data, and edited the manuscript. S R, S H selected donors, provided BM samples and clinical information. M O provided materials and edited the manuscript. I K J K analyzed results and interpreted the data. S S interpreted the data, performed statistical analysis, and edited the manuscript. S G contributed to the study design, provided materials, drafted, and edited the manuscript. D L W interpreted data, drafted, and edited the manuscript. A C K supervised the study, interpreted data, and edited the manuscript. H D V designed and led the study, interpreted data, and edited the manuscript. All authors discussed, commented on, and approved the manuscript in its final form.

Funding

This study was funded by Berlin Institute of Health (BIH) HSCE platform (R S, H D V), the BIH Hub Organoids (S M, N M D) and the Einstein Foundation

Kickbox program (N M D, S M). This project has received funding from the European Union's Horizon 2020 research and innovation program under Grant Agreement No. 825392 (ReSHAPE-h2020.eu), the grant agreement no. 101057438 (geneTIGA-horizon.eu), and the Grant Agreement No. 101054501 (ERC-2021-ADG). Views and opinions expressed are however those of the author(s) only and do not necessarily reflect those of the European Union or the European Health and Digital Executive Agency (HADEA). Neither the European Union nor the granting authority can be held responsible for them. This study was also partially supported by German Research Foundation (DFG) through funding of the Collaborative Research Centre 1444 (N M D, S R, S G, M R K, M O, H D V) and German Federal Ministry of Education and Research (BMBF) under Grant Agreement 161L0234B (BOAC).

The funders had no role in study design, data collection and analysis, decision to publish, or preparation of the manuscript.

Institutional review board statement

The recruitment of study subjects was conducted in accordance with the Ethics Committee of Charité—Universitätsmedizin Berlin in compliance with the Declaration of Helsinki (EA1/090/21).


Informed consent statement

Human adult bone marrow trabecular bone samples were obtained after informed consent from patients treated at the Center for Musculoskeletal Surgery Charité—Universitätsmedizin (Berlin, Germany).

ORCID iDs

Stefania Martini  <https://orcid.org/0000-0002-3084-3514>

Norman Michael Drzeniek  <https://orcid.org/0000-0001-6562-2351>

Matthias Reiner Kollert  <https://orcid.org/0000-0001-8193-9631>

Stephan Schlickeiser  <https://orcid.org/0000-0003-3142-2890>

Dimitrios Laurin Wagner  <https://orcid.org/0000-0002-2189-3579>

References

- [1] Lucas D 2021 Structural organization of the bone marrow and its role in hematopoiesis *Curr. Opin. Hematol.* **28** 36–42
- [2] Fröbel J, Landsperky T, Percin G, Schreck C, Rahmig S, Ori A, Nowak D, Essers M, Waskow C and Oostendorp R A J 2021 The hematopoietic bone marrow niche ecosystem *Front. Cell Dev. Biol.* **9** 705410
- [3] Nutt S L, Hodgkin P D, Tarlinton D M and Corcoran L M 2015 The generation of antibody-secreting plasma cells *Nat. Rev. Immunol.* **15** 160–71
- [4] Glaser D E, Curtis M B, Sariano P A, Rollins Z A, Shergill B S, Anand A, Deely A M, Shirure V S, Anderson L and Lowen J M 2020 Organ-on-a-chip model of vascularized human bone marrow niches *Bioengineering* **280** 121245
- [5] Khan A O et al 2023 Human bone marrow organoids for disease modeling, discovery, and validation of therapeutic targets in hematologic malignancies *Cancer Discovery* **13** 364–85
- [6] Chen J, Hendriks M, Chatzis A, Ramasamy S K and Kusumbe A P 2020 Bone vasculature and bone marrow vascular niches in health and disease *J. Bone Min. Res.* **35** 2103–20
- [7] Khodadadi L, Cheng Q, Radbruch A and Hiepe F 2019 The maintenance of memory plasma cells *Front. Immunol.* **10** 721
- [8] Lightman S M, Utley A and Lee K P 2019 Survival of long-lived plasma cells (LLPC): piecing together the puzzle *Front. Immunol.* **10** 965
- [9] Rösel A L et al 2015 Classification of common variable immunodeficiencies using flow cytometry and a memory B-cell functionality assay *J. Allergy Clin. Immunol.* **135** 198–208.e5
- [10] Mikkilineni L and Kochenderfer J N 2021 CAR T cell therapies for patients with multiple myeloma *Nat. Rev. Clin. Oncol.* **18** 71–84
- [11] Johnson C B, Zhang J and Lucas D 2020 The role of the bone marrow microenvironment in the response to infection *Front. Immunol.* **11** 585402
- [12] Aoki K et al 2021 Identification of CXCL12-abundant reticular cells in human adult bone marrow *Br. J. Haematol.* **193** 659–68
- [13] Jourdan M, Cren M, Robert N, Bolloré K, Fest T, Duperray C, Guilloton F, Hose D, Tarte K and Klein B 2014 IL-6 supports the generation of human long-lived plasma cells in combination with either APRIL or stromal cell-soluble factors *Leukemia* **28** 1647–56
- [14] Shah N, Chari A, Scott E, Mezzi K and Usmani S Z 2020 B-cell maturation antigen (BCMA) in multiple myeloma: rationale for targeting and current therapeutic approaches *Leukemia* **34** 985–1005
- [15] Jansen L E, Birch N P, Schiffman J D, Crosby A J and Peyton S R 2015 Mechanics of intact bone marrow *J. Mech. Behav. Biomed. Mater.* **50** 299–307
- [16] Winer J P, Oake S and Janmey P A 2009 Non-linear elasticity of extracellular matrices enables contractile cells to communicate local position and orientation *PLoS One* **4** e6382
- [17] Braham M V J, van Binnendijk R S, Buisman A-M-M, Mebius R E, de Wit J and van Els C A C M 2023 A synthetic human 3D in vitro lymphoid model enhancing B-cell survival and functional differentiation *iScience* **26** 105741
- [18] Wu D et al 2022 A 3D-bioprinted multiple myeloma model *Adv. Healthcare Mater.* **11** 2100884
- [19] Harmon K A, Roman S, Lancaster H D, Chowhury S, Cull E, Goodwin R L, Arce S and Fanning S 2022 Structural and ultrastructural analysis of the multiple myeloma cell niche and a patient-specific model of plasma cell dysfunction *Microsc. Microanal.* **28** 254–64
- [20] Qazi T H, Mooney D J, Duda G N and Geissler S 2020 Niche-mimicking interactions in peptide-functionalized 3D hydrogels amplify mesenchymal stromal cell paracrine effects *Biomaterials* **230** 119639
- [21] Qazi T H, Mooney D J, Duda G N and Geissler S 2017 Biomaterials that promote cell-cell interactions enhance the paracrine function of MSCs *Biomaterials* **140** 103–14
- [22] Lourenço D, Lopes R, Pestana C, Queirós A C, João C and Carneiro E A 2022 Patient-derived multiple myeloma 3D models for personalized medicine—are we there yet? *Int. J. Mol. Sci.* **23** 12888
- [23] Santos Rosalem G, Gonzáles Torres L A, de Las Casas E B, Mathias F A S, Ruiz J C and Carvalho M G R 2020 Microfluidics and organ-on-a-chip technologies: a systematic review of the methods used to mimic bone marrow *PLoS One* **15** e0243840

- [24] Kefallinou D, Grigoriou M, Boumpas D T, Gogolides E and Tserepi A 2020 Fabrication of a 3D microfluidic cell culture device for bone marrow-on-a-chip *Micro Nano Eng.* **9** 100075
- [25] Drzeniek N M *et al* 2021 Bio-instructive hydrogel expands the paracrine potency of mesenchymal stem cells *Biofabrication* **13** 045002
- [26] Chaudhuri O *et al* 2016 Hydrogels with tunable stress relaxation regulate stem cell fate and activity *Nat. Mater.* **15** 326–34
- [27] Bankhead P *et al* 2017 QuPath: open source software for digital pathology image analysis *Sci. Rep.* **7** 16878
- [28] Sarkis R *et al* 2023 MarrowQuant 2.0: a digital pathology workflow assisting bone marrow evaluation in experimental and clinical hematology *Mod. Pathol.* **36** 100088
- [29] Misra S, Moro C F, Del Chiaro M, Pouso S, Sebestyén A, Löhr M, Björnstedt M and Verbeke C S 2019 *Ex vivo* organotypic culture system of precision-cut slices of human pancreatic ductal adenocarcinoma *Sci. Rep.* **9** 2133
- [30] Kang C, Qiao Y, Li G, Baechle K, Camelliti P, Rentschler S and Efimov I R 2016 Human organotypic cultured cardiac slices: new platform for high throughput preclinical human trials *Sci. Rep.* **6** 28798
- [31] Gu Y, Forget A and Shastri V P 2022 Biobridge: an outlook on translational bioinks for 3D bioprinting *Adv. Sci.* **9** 2103469
- [32] Zhang B, Li Y, Wang G, Jia Z, Li H, Peng Q and Gao Y 2018 Fabrication of agarose concave petridish for 3D-culture microarray method for spheroids formation of hepatic cells *J. Mater. Sci., Mater. Med.* **29** 49
- [33] Drzeniek N M, Kahwaji N, Schlickeiser S, Reinke P, Geißler S, Volk H-D and Gossen M 2023 Immuno-engineered mRNA combined with cell adhesive niche for synergistic modulation of the MSC secretome *Biomaterials* **294** 121971
- [34] Saxena A and Wu D 2016 Advances in therapeutic Fc engineering—modulation of IgG-associated effector functions and serum half-life *Front. Immunol.* **7** 580
- [35] Wols H A M, Underhill G H, Kansas G S and Witte P L 2002 The role of bone marrow-derived stromal cells in the maintenance of plasma cell longevity *J. Immunol.* **169** 4213–21
- [36] Cocco M, Stephenson S, Care M A, Newton D, Barnes N A, Davison A, Rawstron A, Westhead D R, Doody G M and Tooze R M 2012 In vitro generation of long-lived human plasma cells *J. Immunol.* **189** 5773–85
- [37] Cornelis R *et al* 2020 Stromal cell-contact dependent PI3K and APRIL induced NF- κ B signaling prevent mitochondrial- and ER stress induced death of memory plasma cells *Cell Rep.* **32** 107982
- [38] Solbu A A, Caballero D, Damigos S, Kundu S C, Reis R L, Halaas Ø, Chahal A S and Strand B L 2023 Assessing cell migration in hydrogels: an overview of relevant materials and methods *Mater. Today Bio* **18** 100537
- [39] Krampe B and Al-Rubeai M 2010 Cell death in mammalian cell culture: molecular mechanisms and cell line engineering strategies *Cytotechnology* **62** 175–88
- [40] Auner H W, Beham-Schmid C, Dillon N and Sabbattini P 2010 The life span of short-lived plasma cells is partly determined by a block on activation of apoptotic caspases acting in combination with endoplasmic reticulum stress *Blood* **116** 3445–55
- [41] Geffroy-Luseau A, Jégo G, Bataille R, Campion L and Pellat-Deceunynck C 2008 Osteoclasts support the survival of human plasma cells *in vitro* *Int. Immunol.* **20** 775–82
- [42] Gomez M R, Talke Y, Goebel N, Hermann F, Reich B and Mack M 2010 Basophils support the survival of plasma cells in mice *J. Immunol.* **185** 7180–5
- [43] Chu V T and Berek C 2012 Immunization induces activation of bone marrow eosinophils required for plasma cell survival: cellular immune response *Eur. J. Immunol.* **42** 130–7
- [44] Baccin C, Al-Sabah J, Velten L, Helbling P M, Grünschläger F, Hernández-Malmierca P, Nombela-Arrieta C, Steinmetz L M, Trumpp A and Haas S 2020 Combined single-cell and spatial transcriptomics reveal the molecular, cellular and spatial bone marrow niche organization *Nat. Cell Biol.* **22** 38–48
- [45] Li H, Bräunig S, Dhapola P, Karlsson G, Lang S and Scheduling S 2022 Single-cell RNA sequencing identifies phenotypically, functionally, and anatomically distinct stromal niche populations in human bone marrow *Blood* **140** 5764–5
- [46] Kegyes D *et al* 2022 Patient selection for CAR T or BiTE therapy in multiple myeloma: which treatment for each patient? *J. Hematol. Oncol.* **15** 78
- [47] Kath J *et al* 2022 Pharmacological interventions enhance virus-free generation of TRAC-replaced CAR T cells *Mol. Ther. Methods Clin. Dev.* **25** 311–30